

Equilibrium tides and magnetic activity in stars with close-by massive planets

The intriguing case of WASP-18

A. F. Lanza and S. N. Breton

INAF-Osservatorio Astrofisico di Catania, Via S. Sofia, 78 - I-95123 Catania, Italy
e-mail: antonino.lanza@inaf.it, sylvain.breton@inaf.it

Received ... ; accepted ...

ABSTRACT

Aims. WASP-18 is an F6V star that hosts a planet with a mass of ~ 10 Jupiter masses and an orbital period of ~ 0.94 days. In spite of its relatively fast rotation and young age, the star remains undetected in X-rays, thus implying a very low level of magnetic activity. To account for such unexpected properties, we propose a mechanism that modifies the internal stratification and the photospheric magnetic activity of a late-type main sequence star with a close-by massive planet based on the action of the equilibrium tide.

Methods. We speculate that the horizontal flow produced by the equilibrium tide may interact with the convective plumes in the overshoot layer below the stellar outer convective envelope. The interaction is characterised by a very high Reynolds number ($Re \sim 10^{10}$), leading to the development of turbulent boundary layers at the surface of such structures, whereas turbulent wakes extend over most of the overshoot layer that they straddle.

Results. We propose that such a tidally induced turbulence can lead to a reduction of the filling factor of the downdrafts in the overshoot layer. As a consequence, the absolute value of the sub-adiabatic gradient increases in that layer hindering the emergence of magnetic flux tubes responsible for the formation of photospheric starspots. We conjecture that this process is occurring in WASP-18, thus providing a possible mechanism to account for the very low level of magnetic activity observed for such a planet host.

Key words. planetary systems – planet-star interactions – Stars: solar-type – Stars: activity – Stars: magnetic fields – Stars: individual: WASP-18 (HD 10069), WASP-12

1. Introduction

Late-type main sequence (MS) stars have an outer convective envelope surrounding a radiative zone. The convective motions in the envelope do not stop at the level where the Schwarzschild criterion for the onset of convection is marginally satisfied, but they overshoot in the radiative zone below because of the inertia of the downwardly directed fluid parcels (e.g. Zahn 1991; Kippenhahn et al. 2013). Convective motions in stellar outer convection zones develop over several pressure scale heights, H_p , and are characterised by extremely large Rayleigh and Reynolds numbers of the order of at least of 10^{25} and $10^{12} - 10^{13}$, respectively (Priest 1984). In such a regime, a strong asymmetry arises between upward and downward convective motions, with the latter taking the form of concentrated downdrafts extending over most of the depth of the convection zone and reaching the lower boundary with a velocity well in excess of that predicted by the mixing-length theory usually adopted to model stellar convection. These downdrafts occupy an area of the order of 10% at the base of the convective envelope, while the upward directed motions are characterised by a wider areal filling factor and lower upward velocities because of the continuity of mass and enthalpy transport (see Rieutord & Zahn 1995).

Convective downdrafts penetrate into the underlying radiative region before being stopped by its stable stratification that strongly hampers motions in the direction of the local gravity (the vertical or radial direction). A model for such a penetrative convection was proposed by Zahn (1991). It shows that

the downdrafts enforce a nearly adiabatic stratification over almost the entire vertical extent of their penetration before being stopped in a terminal layer of a few kilometers thickness below which the stratification becomes strongly sub-adiabatic as in the absence of penetrative convection. The mean extension of the penetration of the downdrafts depends on a free parameter in Zahn's model and it is usually assumed to be of the order of $(0.1 - 0.2) H_p$ at the base of the convection zone, although recent numerical simulations have shown that it depends on the density gradient at the interface between the convection zone and the radiative zone and on the stellar rotation that affects downdrafts through the effect of the Coriolis force (cf. Korre & Featherstone 2021, and references therein). The statistics of the plume penetration has been analysed by Pratt et al. (2017) and subsequently by Baraffe et al. (2021) and Baraffe et al. (2023) by means of numerical simulations of stellar convection.

The stratification induced by the downdrafts in the overshoot layer is slightly sub-adiabatic $\nabla - \nabla_{ad} < 0$ ¹ (cf. Sect. 5 of Zahn 1991). For the typical ranges of adopted parameters, the sub-adiabatic gradient is $|\nabla - \nabla_{ad}| \sim 10^{-6} - 10^{-5}$ in Sun-like stars. This strongly reduces the buoyancy instability of horizontal magnetic fields thus making the overshoot layer a candidate for the storage of the intense magnetic fields (up to ~ 10 T) that are invoked by some models to account for the solar and stellar magnetic

¹ The temperature gradients are defined as $\nabla_{ad} = (\partial \ln T / \partial \ln P)_{ad}$ at constant entropy and $\nabla = \partial \ln T / \partial \ln P$ in the actual internal stratification (cf. Kippenhahn et al. 2013).

activity, in particular, for the formation of sunspots (e.g. Caligari et al. 1995, see also Sect. 2).

The overshoot layer is relevant not only as a potential storage site for intense magnetic fields, but it plays an active and relevant role in the internal stellar dynamics. It is the layer where the downdrafts can excite gravity waves that contribute to the transport of angular momentum in addition to those excited by turbulent convection at the base of the convective envelope (e.g. Zahn et al. 1997; Lecoanet & Quataert 2013; Alvan et al. 2014; Pinçon et al. 2016; Breton et al. 2022). Moreover, penetrative convection contributes to the internal mixing leading to the burning of light elements such as lithium, boron, and beryllium (e.g. Montalbán & Schatzman 2000).

The overshoot layer is regarded as coincident with most of the solar (and stellar) tachocline, namely, the layer where a strong radial gradient of the rotation velocity is localised, at the interface between the rigidly rotating radiative interior and the differentially rotating convection zone (Schou et al. 1998). The origin of the solar tachocline is still strongly debated with hydrodynamical models essentially relying on the proposal by Spiegel & Zahn (1992), invoking a strongly anisotropic turbulent viscosity in the layer, while magnetohydrodynamics models mainly rely on dynamo-generated oscillating magnetic fields (cf. Barnabé et al. 2017) since numerical simulations showed the difficulty in confining the shear in the presence of a fossil stationary magnetic field in the radiative zone (e.g. Brun & Zahn 2006; Strugarek et al. 2011).

In the present work, we investigate a possible effect of the equilibrium tide on the convective downdrafts in a late-type MS star that has a close-by massive companion in the case when stellar rotation is not synchronised with the orbital motion. Our investigation has been inspired by the intriguing observational results concerning the stellar activity of WASP-18 that hosts a planet with a mass of ~ 10 Jupiter masses orbiting in only 0.941 days (Hellier et al. 2009). Such a star was noticed as a member of the group of hosts of massive transiting planets having a very low level of chromospheric activity as measured by the $\log R'_{\text{HK}}$ index based on the Ca II H&K resonance line core emission (cf. Fig. 2 of Fossati et al. 2013). The proposed explanation for such a missing or strongly depressed emission in the core of chromospheric lines is an absorption by a circumstellar torus of material formed by the strong evaporation of the planetary atmosphere because of their proximity to their host stars (cf. Haswell et al. 2012; Lanza 2014; Fossati et al. 2015).

A prediction of the absorbing torus model is that the X-ray emission observed in these planetary hosts should be that expected on the basis of their rotation rate and age. The reason is that the torus is virtually transparent at wavelengths below ~ 35 nm, thanks to the proportionality of the bound-free absorption cross section of Hydrogen to the third power of the wavelength. Given the quite fast rotation of WASP-18 ($v \sin i \sim 11 \text{ km s}^{-1}$, corresponding to a minimum rotation period $P_{\text{rot}} \sim 5.6$ days) and an estimated age of $\sim 0.6 - 0.8$ Gyr (Hellier et al. 2009), its non-detection at X-ray wavelengths by Pillitteri et al. (2014) came as a big surprise. Their X-ray luminosity upper limit was two orders of magnitude below the expected level making Pillitteri et al. speculate that the massive close-by companion of WASP-18 can somehow hinder its magnetic activity. Subsequent observations in the extreme ultraviolet (EUV) with the Hubble Space Telescope by Fossati et al. (2018) confirmed the suppressed level of magnetic activity also in the EUV emission lines coming from the upper chromosphere and the transition region of the stellar atmosphere, reinforcing its peculiarity and the need for an explanation.

Recently, Pillitteri et al. (2023) observed KELT-24, a star very similar to WASP-18 in age and effective temperature, hosting a more distant hot Jupiter, and found it to show the level of X-ray emission predicted on the basis of its young age. A similar level of X-ray emission was observed in other planetary hosts with similar spectral types (cf. Fig. 7 of Pillitteri et al. 2023). Moreover, KELT-24 shows a significantly higher mean energy of the optical flares than WASP-18, a result based on the observations performed by the Transit Exoplanet Survey Satellite (TESS; Ricker et al. 2015), thus confirming an unexpected low level of magnetic activity in our target.

A possible explanation for the low level of activity of WASP-18 could be that we have caught the star in a grand minimum of activity such as those affecting the Sun for about 15% of the time (e.g. Biswas et al. 2023). Our knowledge of similar phenomena in other stars is extremely limited (cf. Baum et al. 2022; Isaacson et al. 2024) and no generally accepted physical mechanism has been proposed for the generation of grand minima, even in the Sun (Karak 2023). Therefore, we decided to look for an alternative explanation, although the possibility that WASP-18 be presently in a grand minimum regime cannot be excluded.

Specifically, we propose here a conjectural model that predicts the disruption of the downdrafts because of the turbulence excited below the convection zone by the motions associated with the equilibrium tide. This leads to a significant increase of the sub-adiabaticity in the layers immediately below the stellar convection zone that can make the buoyancy instability of magnetic fields stored there much more difficult. This hinders the formation of starspots in the stellar photosphere resulting in a strong reduction of stellar magnetic activity and offering a potential explanation for the very low level of activity observed in WASP-18.

2. Model

2.1. Overshoot layer and hydromagnetic dynamos in late-type stars

The overshoot layer has been proposed as a seat for the storage of large amount of magnetic flux in late-type stars. Even if the main stellar hydromagnetic dynamo works in the bulk of the convection zone as suggested by recent numerical simulations (e.g. Brun & Browning 2017; Käpylä et al. 2023) and the overshoot layer may not play a universal role in the amplification and modulation of the stellar magnetic field as discussed, for instance, in Sect. 8.4 of Charbonneau (2020), we speculate that the overshoot layer plays a relevant role for the dynamo action in the case of F-type stars such as WASP-18.

The larger velocities of convective motions in F-type stars with respect to G- and K-type stars (Brun et al. 2017; Corsaro et al. 2021) can lead to the formation of stronger downdrafts as seen in the numerical simulations of, for example, Breton et al. (2022). These can effectively pump most of the magnetic flux produced by a dynamo from the bulk of the convection zone into the overshoot layer (e.g. Tobias et al. 1998, 2001) that we assume to coincide with the stellar tachocline. Thanks to the tachocline shear, the magnetic field in the overshoot layer can be remarkably amplified, thus contributing most of the magnetic flux responsible for stellar activity, in particular, for photospheric starspots.

An important finding is that a dynamo model with an overshoot layer is capable of producing a more stable modulation with longer cycles than a dynamo model restricted to the convection zone (Guerrero et al. 2016; Käpylä et al. 2023). This

seems to be in closer agreement with the persistent decadal activity cycles observed in stars with a radiative interior in contrast to the more chaotic activity displayed by fully convective stars.

Another class of dynamo models that could be relevant for WASP-18 is that proposed to operate close to the top of the convection zone, precisely in a near surface shear layer (Böhm-Vitense 2007; Brandenburg et al. 2017) akin to that found by helioseismology in the Sun (Schou et al. 1998). Assuming that such a near-surface dynamo is operating in WASP-18, we predicted a negligible effect of the tidal flow on it because the tidal shear is at least one to two orders of magnitude smaller than the radial shear, assuming the latter to be similar to that observed in the Sun (see Sect. 2.3 for a quantification of the tidal shear and, for the near surface shear, Berekat et al. 2014). Moreover, the curl of the equilibrium tidal flow vanishes in the convection zone (Ogilvie 2014), thereby preventing the equilibrium tide from affecting the α effect of the dynamo in the convection zone. In other words, we do not expect tides to be capable of significantly affect or quench a near surface dynamo, when it is indeed at work. Similarly, we do not expect that the equilibrium tide can produce any relevant perturbation of the shaping action of the sub-surface shear layer on the magnetic fields generated in the bulk of the convection zone (Pipin & Kosovichev 2011; Brandenburg et al. 2023).

Nevertheless, a near-surface dynamo is likely not capable of amplifying the magnetic field as effectively as a dynamo storing the toroidal field in the overshoot layer because the strong superadiabaticity in near surface layers makes a comparable toroidal field strongly unstable to buoyancy there. Moreover, the observed solar meridional flow is poleward in the upper half of the solar convection zone, thus leading to a reduced or reversed migration of the active regions with respect to the observed butterfly diagram in the Sun, if the toroidal field generation is dominated by a near-surface solar dynamo (see e.g. Cloutier et al. 2023, for the role played by the helioseismically determined meridional circulation in a Babcock-Leighton model of the solar cycle). For such reasons, we focus our investigation on dynamos where the overshoot layer below the convection zone plays a crucial role contributing most of the magnetic flux responsible for stellar activity. Such dynamos have the advantage of storing strong toroidal magnetic fields (≥ 10 T) in the subadiabatic overshoot layer. These fields can emerge at low latitudes in the Sun producing the active regions observed during the maximum and decay phase of the solar cycle. On the other hand, dynamos storing the toroidal fields in the deepest layers of the superadiabatic convection zone, such as Babcock-Leighton dynamos (Charbonneau 2020; Cloutier et al. 2023), are generally limited to weaker fields ($\sim 10^4$ G), that lead to active regions formation only at high latitudes ($\geq 30^\circ - 40^\circ$) in the Sun (cf. Caligari et al. 1995).

2.2. Downdrafts and sub-adiabatic stratification in the overshoot layer

The penetrative convection below the convective zone has been described as consisting of downward turbulent plumes (or down-drafts) by Rieutord & Zahn (1995). Their model was extended in Sect. 3 of Pinçon et al. (2016) and we adopt it here to estimate the relevant parameters of the convective downdrafts. Considering an horizontal section of a plume, its downward directed mean velocity is expressed by Pinçon et al. (2016) by a Gaussian profile with a standard deviation (effective radius of the downdraft):

$$b = \frac{z_0}{\sqrt{2}} \frac{3\alpha_E(\Gamma_1 - 1)}{2\Gamma_1 - 1}, \quad (1)$$

where z_0 is the depth of the convection zone, $\alpha_E = 0.083$ is a universal coefficient derived from laboratory studies and simulations of penetrative convection (cf. Sect. 3.2 of Pinçon et al. 2016), and Γ_1 is the ratio of the specific heats at constant pressure and volume, that is, $\Gamma_1 = 5/3$ in the fully ionised layers in the interior of a solar-like star. The typical value of the downdraft cross-sectional size b is between 5×10^6 and 10^7 m in late-type MS stars. The total number of plumes \mathcal{N} simultaneously present at the base of the convection zone is of the order of $\sim 10^3$ according to Rieutord & Zahn (1995), which implies an areal filling factor $f \sim 0.1$.

The downward directed plume velocity has been estimated by assuming that the downdrafts transport all the stellar convective flux as in Sect. 3 of Rieutord & Zahn (1995). In such a way, their velocity at the top of the overshoot layer is given by (cf. Eq. (25) of Pinçon et al. 2016):

$$V_b = \left(\frac{2L}{\pi\rho_b r_b^2} \right)^{1/3}, \quad (2)$$

where L is the luminosity of the star, ρ_b the density at the base of the convection zone, and $r_b = R - z_0$ the radius of that layer with R the radius of the star. Adopting the model by Zahn (1991), the plume velocity depends on the depth z as measured from the level $r = r_b$ according to

$$V(z) = V_b \left[1 - \left(\frac{z}{L_p} \right)^2 \right]^{1/3}, \quad (3)$$

where L_p is the depth down to which the plume penetrates, that is, the depth of the overshoot layer. Here it is assumed to be $0.1 H_p$, where H_p is the pressure scale height at the base of the convection zone (see Korre & Featherstone 2021, for a discussion of its dependence on stellar parameters including the effect of rotation). However, the possibility of a deeper convective penetration, down to $\sim 0.5 H_p$, cannot be excluded according to the results by Anders et al. (2022) who discussed the difficulties for a proper numerical simulation of overshooting convection in stars.

The mean lifetime of the convective downdrafts τ_p is the most uncertain parameter. Nevertheless, following the arguments in Sect. 3.4 of Pinçon et al. (2016), it seems reasonable to assume it of the order of the convective turnover time at the base of the stellar convection zone, that is,

$$\tau_p \sim \alpha_{\text{mlt}} H_p / v_c, \quad (4)$$

where α_{mlt} is the ratio of the mixing length to the local pressure scale height H_p , while v_c is the velocity of convective motions at the base of the convection zone as given by the standard mixing-length theory (cf. Ch. 7 of Kippenhahn et al. 2013).

The time evolution of the downdrafts is uncertain as well. It has been discussed by Pinçon et al. (2021) who considered two limiting cases where their velocity field varies as $\exp(-t^2/\tau_p^2)$ or $\exp(-t/\tau_p)$, respectively. The former Gaussian time dependence corresponds to a rapid damping of the downdrafts, while the latter exponential implies a slower decay and a longer duration. We adopted the exponential decay law because we are interested in the case of relatively long-lived downdrafts. Moreover, this assumption allows us to easily add the effect of the turbulent diffusivity on their evolution (cf. Sect. 2.8).

In conclusion, we consider the following vertical velocity field for our downdrafts:

$$\mathbf{v}_{\text{down}}(s, z, t) = V(z) \exp\left[-\left(\frac{t}{\tau_p}\right)\right] \exp\left[-\left(\frac{s^2}{2b^2}\right)\right] \hat{\mathbf{z}}, \quad (5)$$

where s is the horizontal distance from the axis of the downdraft assumed to be cylindrically symmetric around its vertical axis (cf. Rieutord & Zahn 1995), $\hat{\mathbf{z}}$ is the unit vector in the vertical direction, $V(z)$ is given by Eq. (3), b is the effective radius of the downdraft as given by Eq. (1), and the time, t , is measured from the starting of the downdraft.

The mean temperature gradient in the overshoot layer down to the level $z \sim L_p$ is given by (cf. Eq. (5.10) in Zahn 1991)

$$\frac{\nabla}{\nabla_{\text{ad}} - \nabla} = \frac{f}{c\chi_p} \frac{V_b H_p}{K}, \quad (6)$$

where f is the filling factor of the downdrafts at the base of the convection zone where $r = r_b$, $c \sim 1 - f$ a geometric coefficient, $\chi_p = (\partial \ln \chi / \partial \ln p)_{\text{ad}}$ is the logarithm derivative of the radiative conductivity, χ , with respect to the plasma pressure p in adiabatic conditions, and $K = \chi / (\rho c_p)$ is the thermal diffusivity with ρ as the density and c_p the specific heat at constant pressure. The radiative conductivity depends on the opacity of the plasma κ as

$$\chi = \frac{16 \sigma T^3}{3 \rho \kappa}, \quad (7)$$

where σ is the Stefan-Boltzmann constant and T the temperature. In the case of the Sun, $\chi_p \sim 1.8$, $K \sim 2 \times 10^3 \text{ m}^2 \text{ s}^{-1}$ (Zahn 1991), $V_b \sim 190 \text{ m s}^{-1}$ (Pinçon et al. 2016), $H_p \sim 5.6 \times 10^7 \text{ m}$, so that $V_b / H_p K \sim 3.5 \times 10^6$. For $\nabla \simeq \nabla_{\text{ad}} = 0.4$ and $f \sim 0.1$, Eq. (6) gives a sub-adiabaticity $\nabla_{\text{ad}} - \nabla \sim 2.5 \times 10^{-5}$.

2.3. Interaction of the equilibrium tide with the downdrafts

The equilibrium tide is the quasi-hydrostatic deformation of the host star under the action of the tidal potential generated by its planet (Remus et al. 2012; Ogilvie 2014; Barker 2020). The relative deformation in the radial direction is of the order of

$$\epsilon(r) \equiv \left(\frac{m_p}{M}\right) \left(\frac{r}{a}\right)^3, \quad (8)$$

where m_p is the mass of the planet, M the mass of the star, r the radial distance from the centre of the star where we consider the tidal deformation, and a the semimajor axis of the orbit assumed to be circular and in the equatorial plane of the star. The tidal deformation ξ in the radiative zone of a star is a solenoidal vector ($\nabla \cdot \xi = 0$) as shown by Ogilvie (2014) in his Sect. 3.2.

The vertical deformation due to the equilibrium tide at a distance r from the centre of the star is $\xi_r \sim \epsilon r$, while the deformation in the azimuthal (horizontal) direction ξ_ϕ follows from $\nabla \cdot \xi = 0$ by considering that the horizontal wavenumber of the tidal deformation is $2/r$ for the semi-diurnal tide at the equator. In other words, we have

$$\xi_\phi \sim 2 \epsilon r. \quad (9)$$

The Eulerian velocity field of the equilibrium tide in a reference frame that rotates with the stellar angular velocity Ω is $\partial \xi / \partial t = \omega_{\text{tide}} \xi$, where ω_{tide} is the frequency of the semi-diurnal tide given by

$$\omega_{\text{tide}} = 2(n - \Omega), \quad (10)$$

where $n \equiv 2\pi/P_{\text{orb}}$ is the orbital mean motion with P_{orb} being the orbital period and $\Omega = 2\pi/P_{\text{rot}}$ the angular velocity of rotation of the star with a rotation period P_{rot} , and we assume $n > \Omega$ for a close-by planet. We consider only the semi-diurnal or quadrupolar equilibrium tide (with spherical degree and azimuthal wavenumbers $l = m = 2$ in Remus's or Ogilvie's notation) because the higher-order tidal terms are much smaller and can be neglected for our purposes.

In the case of the massive very hot Jupiter of WASP-18, with $a = 0.02014 \text{ au}$, $m_p = 10.06$ Jupiter masses, $M = 1.22 M_\odot$, $P_{\text{rot}} \sim 5.6$ days, $P_{\text{orb}} = 0.941$ days, and $r_b/R = 0.844$ with $R = 1.21 R_\odot$ being the star radius (cf. Sect. 3.1), we obtain $\epsilon(r_b) \equiv \epsilon_b = 1.0 \times 10^{-4}$ and $\omega_{\text{tide}} = 1.28 \times 10^{-4} \text{ s}^{-1}$. Hence, the azimuthal relative tidal velocity between a downdraft and the surrounding plasma in the overshoot layer turns out to be $\xi_\phi \sim 18 \text{ m s}^{-1}$.

The shear associated with the equilibrium tide is too small to produce a linear instability leading to turbulence (Seguin 1976; Zahn 1977, Sect. 4e). Therefore, the tidal flow is generally assumed to be laminar, except in the cases when the tide enters into a parametric resonance with inertial waves (cf. Sect. 4.1 of Ogilvie 2014, the so-called elliptic instability) or gravity waves in the deep radiative interior (Vidal et al. 2019; Weinberg et al. 2012). If such a resonance occurs, the resulting nonlinear instability can lead to a turbulent flow that increases the dissipation by many orders of magnitude. However, none of these situations occurs in the system of WASP-18. Specifically, the elliptic instability requires $-1 < n/\Omega < 3$, a condition that is not verified in this system where $n/\Omega \sim 5.5$. On the other hand, $n/\Omega \sim 5.5$ could allow a resonance with gravity waves in the deep radiative interior where the Brunt-Väisälä frequency $N \gtrsim (8 - 10)\Omega$ as illustrated in Fig. 2 of Vidal et al. (2019). Although the Brunt-Väisälä frequency N increases very rapidly with depth below the top of the radiative zone, the layers where such a resonance can occur are probably located much deeper than the overshoot layer; thus, the resulting turbulence cannot affect the layer we are interested in. Similarly, any resonance with inertial waves can be excluded in WASP-18 because those waves cannot be excited in the interior of our target given that the tidal frequency is greater than twice its angular velocity of rotation (Ogilvie & Lin 2007).

We conjecture that the establishment of a turbulent flow in the overshoot layer can be related to a different mechanism that depends on the interaction between the vertical convective plumes that straddle the layer and the horizontal tidal flow in the azimuthal direction that is orthogonal to them. We assume that the mean velocity field of the downdrafts is not modified by the presence of the equilibrium tide. We regard each downdraft as a rigid structure, that is, a vertical obstacle to the horizontal flow of the equilibrium tide. The rigidity of the downdrafts is due to the presence of a relatively strong vertical magnetic field in the downdrafts as seen in numerical simulations of penetrative convection and magnetic flux pumping into the overshoot layer (see e.g. Fig. 2 of Tobias et al. 1998). Such a field is produced by the amplification, owing to the vertical shear in a downdraft, of a weaker field in the overlying convection zone that is provided by an hydromagnetic dynamo operating there. Since the downdraft velocity is of the order of hundreds of meters per second (see Sects. 2.2 and 3.1), the vertical magnetic field in a downdraft has an energy density about two orders of magnitude larger than the kinetic energy density of the horizontal tidal flow ξ_ϕ that is only of the order of tens of meters per second. Therefore, such a vertical magnetic field cannot be significantly distorted by the tidal flow and the magnetised plasma of the downdraft provides an obstacle to the tidal flow.

In Fig. 1, we provide a sketch of our system with the magnetised plumes shown as blue rigid vertical cylinders of diameter $2b$, while the horizontal yellow planes indicate the base of the convection zone (top) and the base of the overshoot layer at a depth L_p below (bottom), respectively. The horizontal red arrows indicate the horizontal flow of the equilibrium tide, while turbulence is sketched as knotted red solid lines around and past only part of one of the cylinders, for simplicity. Both the turbulent boundary layer and the turbulent wake are schematically indicated. We note that although turbulent flow lines have been drawn for only a small part of the domain, the turbulence extends itself over the whole overshoot layer because of the very high Reynolds number of such a system (see Sect. 2.4).

An additional process occurring in the overshoot layer is the formation of a more or less uniform horizontal layer of magnetic field owing to the pumping effect of the downdrafts. We expect such a magnetised layer to be located in the lower part of the overshoot domain, not far from the terminal layer where the downdrafts are braked by the stratification of the underlying radiative zone. This is because the downdrafts themselves are capable of pushing the field down to that level. In other words, we assume that the upper part of the overshoot layer is devoid of any horizontal magnetic field and possesses only the vertical fields associated with the downdrafts. Therefore, in the upper part of the overshoot layer, the turbulence around the downdrafts cannot be quenched by the horizontal magnetic field.

2.4. Stationary and oscillating horizontal flows

It is useful to consider an analogous system consisting of an array of vertical rigid indefinite circular cylinders placed in a flow perpendicular to their axes of symmetry that is produced by the equilibrium tide. Let us first consider the case of a uniform and steady perpendicular flow. In this system, the Reynolds number is defined as $Re = DU/\nu$, where D is the diameter of each cylinder, U the speed of the flow at infinity, and ν the kinematic viscosity of the fluid. The kinematic microscopic viscosity below the solar convection zone is $\nu \sim 3 \times 10^{-3} \text{ m}^2 \text{ s}^{-1}$ (cf. Table 1 of Brun & Zahn 2006); assuming $D \sim 2b \sim 10^7 \text{ m}$ and $U \sim \dot{\xi}_\phi \sim 18 \text{ m s}^{-1}$, we obtain $Re \sim 6 \times 10^{10}$ that corresponds to a hydrodynamic regime with a strongly developed turbulence. For comparison, the appearance of turbulence in the wake of the flow past a single indefinite cylinder occurs for $Re \gtrsim 400$, while the turbulence fully develops in the boundary layer at the surface of the cylinder for $Re \gtrsim 5 \times 10^5$ (e.g. Zdravkovich 1997). Williamson (1996) reported that, although for $Re > 10^5 - 10^7$ a uniform fully turbulent wake is expected, a periodic turbulent vortex shedding is observed as typically found in cylinder wakes at $Re \sim 10^3 - 10^4$. The vortex shedding frequency ω_{vs} enters into the definition of the non-dimensional Strouhal number $S_n \equiv \omega_{vs} D/U$ that reaches an asymptotic value of $\sim 0.20 - 0.25$ with increasing Reynolds number Re .

When the flow orthogonal to the axis of a cylinder is oscillating as in the case of the equilibrium tidal flow, a significant change in the above stationary picture occurs when the frequency of the flow oscillation or its first harmonic come close to the natural shedding frequency ω_{sv} corresponding to the asymptotic value of the Strouhal number. In such a case, the shedding frequency tends to lock to the oscillation frequency of the flow and the coherence lengthscale along the wake can increase remarkably (cf. Bearman 1984; Khodkar et al. 2021). However, such a resonant regime is not approached in the case of WASP-18 because the natural shedding frequency for a cylinder of radius $\sim 6.6 \times 10^6 \text{ m}$ in a flow of velocity $U \sim 18 \text{ m s}^{-1}$ is

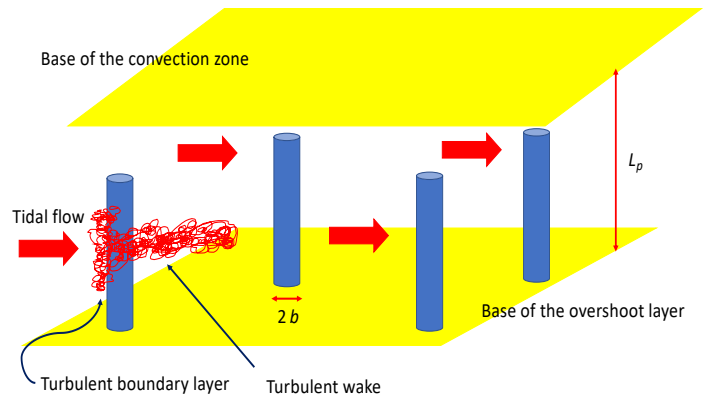


Fig. 1. Cartoon showing the convective downdrafts in the overshoot layer and the turbulence produced by the horizontal tidal flow moving past them in the layer.

$\omega_{vs} \sim 3 \times 10^{-7} \text{ s}^{-1}$ for an asymptotic Strouhal number $S_n = 0.25$, while the tidal frequency is higher by three orders of magnitude being $\omega_{\text{tide}} \sim 1.3 \times 10^{-4} \text{ s}^{-1}$. Therefore, we do not expect any significant modification in the cylinder wake due to the periodic oscillations of the tidal flow.

In the present model, the motivation for treating the downdrafts as obstacles to the tidal flow is the presence of a vertical magnetic field in the downdrafts themselves with an intensity larger than the equipartition strength corresponding to the tidal flow. However, it is interesting to investigate the interaction between the tidal flow and the downdrafts also adopting a different viewpoint that does not rely on the presence of a strong vertical magnetic field in the downdrafts.

Specifically, we consider the linear modelling of the interaction between a columnar vortex and an incoming wave by Dandoy et al. (2023). Convective downdrafts in rotating stars are places of vorticity amplification due to the vertically directed velocity of the plasma that increases with depth in the overlying convection zone. Therefore, we expect that our downdrafts behave similarly to vortices in the overshoot layer. An incident planar wave excites oscillations of a vortex with its characteristic frequency that lead to the radiation of waves from the vortex. Those waves have cylindrical symmetry in the far field and carry between 10% and 20% of the energy of the incident wave depending on whether resonant or neutral oscillation modes are excited in the vortex.

In our case, each downdraft becomes a source of cylindrical waves that can interact nonlinearly with each other producing a turbulent energy cascade (e.g. Nazarenko 2011). The turbulent viscosity produced by such a process should be evaluated by a nonlinear model of the wave excitation and interaction; however, it should be comparable within one order of magnitude with our estimate (given in Sect. 2.5). This is based on the fact that the energy of the interacting waves can reach 0.1 – 0.2 times the energy of the incident tidal wave, while their wavelength is at least comparable with the mean radius of the vortices (Dandoy et al. 2023).

2.5. Turbulence in the overshoot layer

The sub-adiabatic stratification of the overshoot layer has a remarkable impact on the turbulence and the turbulent diffusiv-

ity that we expect to develop inside it as a consequence of the interaction between the downward directed convective plumes and the equilibrium tidal flow. The stable stratification strongly hampers motions in the direction of the local gravity, while the motions over planes perpendicular to the gravity are constrained by the Coriolis force (e.g. Mathis et al. 2018). This leads to an anisotropic turbulent viscosity whose value in the horizontal direction is larger than in the vertical direction.

The turbulent diffusivity in the horizontal direction can be written as

$$\nu_{\text{turb h}} \sim \ell u', \quad (11)$$

where ℓ is the lengthscale of the horizontal turbulence, that is, in the plane perpendicular to the local acceleration of gravity, while u' is the turbulent velocity in the same horizontal plane that comes from the interaction between the vertical downdrafts and the tidal horizontal flow. In the next subsection, we make educated guesses on ℓ taking into account the effect of the Coriolis force that limits the horizontal size of the turbulent eddies. After having estimated the horizontal component of the turbulent diffusivity, we estimate its vertical counterpart $\nu_{\text{turb v}}$ by means of the anisotropic turbulence model by Mathis et al. (2018) that generalises a previous quasi-linear model by Kitchatinov & Brandenburg (2012).

2.6. Length scale of the horizontal turbulent motions

The velocity field \mathbf{u} in the overshoot layer outside the convective plumes can be written as

$$\mathbf{u} = \mathbf{u}_0 + \mathbf{u}', \quad (12)$$

where \mathbf{u}_0 is the tidal velocity field and \mathbf{u}' the turbulent velocity field produced by the interaction of the tidal flow with the penetrating plumes because of its very large Reynolds number (cf. Sects. 2.3 and 2.4). We approximate the turbulent velocity field as a 2D field in the local horizontal plane, that is, the plane orthogonal to the local gravity.

In order to estimate the length scale of this horizontal turbulence, we start from the momentum equation in a rotating reference frame

$$\frac{\partial \mathbf{u}}{\partial t} + (\mathbf{u} \cdot \nabla) \mathbf{u} = -\frac{1}{\rho} \nabla p + 2\boldsymbol{\Omega} \times \mathbf{u} + \nabla \Phi + \nabla \Psi, \quad (13)$$

where t is the time, ρ the plasma density, p the pressure, $\boldsymbol{\Omega}$ the angular velocity of rotation of the reference frame, Φ the gravitational potential of the star, and Ψ the tidal potential (cf. Ogilvie 2014, § 2.1). For simplicity, we assume that the star is rotating with a uniform angular velocity $\boldsymbol{\Omega}$, neglect the viscous force because of the very large Reynolds number, and the Lorentz force by assuming that the dynamical effects of the magnetic fields are small outside the downdrafts (cf. the final paragraph of Sect. 2.3).

To treat the turbulent velocity field, we introduce an ensemble mean indicated with angular brackets and assume that $\langle \mathbf{u}_0 \rangle = \mathbf{u}_0$ and $\langle \mathbf{u}' \rangle = 0$, so that $\langle \mathbf{u} \rangle = \mathbf{u}_0$. Moreover, we assume that the ensemble mean commutes with the time derivative, that implies $\langle \partial \mathbf{u}' / \partial t \rangle = \partial \langle \mathbf{u}' \rangle / \partial t = 0$, and with the spatial derivatives.

The equilibrium tidal flow \mathbf{u}_0 is not an exact solution of the momentum equation, but it is an approximation computed by assuming that the star is capable of adjusting its stratification to the time-varying tidal potential with a very small lag, that is, with a small deviation from the hydrostatic equilibrium (e.g. Ogilvie

2014; Barker 2020). In other words, we may write an equation for the equilibrium tidal flow in the form

$$\frac{\partial \mathbf{u}_0}{\partial t} + (\mathbf{u}_0 \cdot \nabla) \mathbf{u}_0 = -\frac{1}{\rho} \nabla p' + \nabla \Phi' + \nabla \Psi, \quad (14)$$

where the prime indicates the perturbation from the hydrostatic equilibrium we have in the absence of tides and that can be written as $-\nabla p + \rho \nabla \Phi = 0$ (cf. Ogilvie 2014, § 3.2). In Eq. (14), the Coriolis force has been neglected which is possible because the tidal frequency ω_{tide} is remarkably larger than the stellar spin frequency Ω given that we are considering planets orbiting very close to slowly rotating late-type stars. Moreover, we neglected the density perturbation by assuming that the tidal displacement $\mathbf{u}_0 \omega_{\text{tide}}^{-1}$ is small in comparison with the density scale height in the overshoot layer and that the tidal velocity is much smaller than the local sound speed, so that $\nabla \cdot \mathbf{u}_0 = 0$.

Subtracting Eq. (14) from Eq. (13), taking the component in the meridional direction \mathbf{e}_θ so that $\mathbf{e}_\theta \cdot \nabla \Phi = 0$, and applying the ensemble mean to average out some of the terms containing the turbulent velocity field, we find

$$\langle (\mathbf{u}' \cdot \nabla) \mathbf{u}' \rangle \cdot \mathbf{e}_\theta = 2 (\boldsymbol{\Omega} \times \mathbf{u}_0) \cdot \mathbf{e}_\theta, \quad (15)$$

that shows how the spatial correlations of the components of the turbulent velocity are ruled by the Coriolis force acting on the mean tidal flow. We note that the Coriolis force has been retained in the momentum equation for the turbulent velocity because the characteristic turbulence time scale may be much longer than the rotation period of the star.

The scalar triple product on the right-hand side of Eq. (15) can be recast as $2 (\boldsymbol{\Omega} \times \mathbf{u}_0) \cdot \mathbf{e}_\theta = -2\boldsymbol{\Omega} \cdot (\mathbf{u}_0 \times \mathbf{e}_\theta) = -2\Omega u_{0\phi} \cos \theta$, where θ is the colatitude measured from the North pole and $u_{0\phi}$ is the component of the tidal flow in the azimuthal direction. In such a way, Eq. (15) becomes

$$\langle (\mathbf{u}' \cdot \nabla) \mathbf{u}' \rangle \cdot \mathbf{e}_\theta = -2\Omega u_{0\phi} \cos \theta. \quad (16)$$

The characteristic length scale ℓ of the turbulent motions in the horizontal plane can be estimated from Eq. (16) by considering that the largest turbulent eddies have a velocity amplitude u' that is comparable with that of the tidal velocity flow u_0 , so that, in order of magnitude,

$$\frac{u'^2}{\ell} \sim 2\Omega u_0 \cos \theta, \text{ with } u' \lesssim u_0. \quad (17)$$

Considering turbulent motions close to the stellar equator, we find $\theta \sim [(\pi/2) - \ell/r]$, where r is the radius of the spherical surface over which we are estimating the turbulent length scale. Therefore, Eq. (17) becomes

$$\frac{u'^2}{\ell} \sim 2\Omega u_0 \frac{\ell}{r}, \quad (18)$$

and assuming that $u' \sim u_0 \sim \omega_{\text{tide}} \xi_\phi$, we finally obtain

$$\ell \sim \left[\left(\frac{\omega_{\text{tide}}}{2\Omega} \right) r \xi_\phi \right]^{1/2}. \quad (19)$$

Given that $\xi_\phi \sim 2\epsilon_b r_b \ll r$, the length scale $\ell \ll r$, that justifies the approximation $\cos \theta = \sin(\ell/r) \sim \ell/r$ adopted in Eq. (18).

2.7. Turbulent diffusivities and downdraft diffusion timescale

By applying the results of the previous Sect. 2.6, the length scale and the typical velocity of the turbulent motions at $r = r_b$ can be estimated. By means of Eq. (11), we obtain an estimate for the horizontal turbulent diffusivity in the overshoot layer as

$$\begin{aligned} \nu_{\text{turb h}} &\sim \omega_{\text{tide}} \xi_\phi \left[\left(\frac{\omega_{\text{tide}}}{2\Omega} \right) r_b \xi_\phi \right]^{1/2} = \\ &= 2\Omega^{-1/2} \omega_{\text{tide}}^{3/2} \epsilon_b^{3/2} r_b^2, \end{aligned} \quad (20)$$

where the horizontal tidal displacement was substituted from Eq. (9). The vertical turbulent diffusivity can be computed from the horizontal diffusivity by applying the model by Mathis et al. (2018). Specifically, the ratio of the two diffusivities is given by their Eq. (41) as

$$\frac{\nu_{\text{turb v}}}{\nu_{\text{turb h}}} = \frac{2\Omega^2}{N^4 \tau^2}, \quad (21)$$

where Ω is the star rotation frequency, N the Brunt-Väisälä frequency, and τ a characteristic time scale of the turbulence. The Brunt-Väisälä frequency is given by

$$N^2 = \frac{g}{H_p} (\nabla_{\text{ad}} - \nabla), \quad (22)$$

where g is the local acceleration of gravity and the other symbols have already been introduced above. Equation (22) is valid when the gradient of the molecular weight can be neglected and the plasma behaves as an ideal gas. Below the convection zone, $N^2 > 0$, indicating a stable stratification where the buoyancy force opposes adiabatic radial displacements of the plasma elements.

The ratio between the two diffusivities as given by Eq. (21) depends on the relative intensities of the two fundamental forces that constrain the turbulent motions in the vertical and the horizontal directions in the stably stratified layers of a rotating star, that is, the buoyancy force, parameterised by the Brunt-Väisälä frequency, and the Coriolis force, parameterised by the stellar rotation frequency, respectively. The characteristic turbulent timescale τ can be identified with the timescale of variation of the velocity of the largest eddies, that is, $\tau \sim \ell/u' \sim \ell/(\omega_{\text{tide}} \xi_\phi)$, where we have approximated the velocity of the largest eddies with the tidal flow velocity. From Eq. (19), we see that $\ell/\xi_\phi \sim \epsilon^{-1/2}$; hence the timescale $\tau \sim \epsilon^{-1/2} \omega_{\text{tide}}^{-1}$ and Eq. (21) can be recast as

$$\frac{\nu_{\text{turb v}}}{\nu_{\text{turb h}}} \sim \frac{2 \epsilon \Omega^2 \omega_{\text{tide}}^2}{N^4}. \quad (23)$$

To illustrate the application of this formula, we consider two different limiting cases. First, we suppose that the downdrafts can penetrate undisturbed below the convection zone and enforce a nearly adiabatic stratification as given by Eq. (6). Assuming, for example, $\nabla_{\text{ad}} - \nabla \sim 10^{-5}$ in the layer and adopting the characteristic parameters at the base of the convection zone of WASP-18 (see Sect. 3.1), that is, $g = 320 \text{ m s}^{-2}$, and $H_p = 4.4 \times 10^7 \text{ m}$, we find $N = 8.5 \times 10^{-6} \text{ s}^{-1}$ and $\nu_{\text{turb v}}/\nu_{\text{turb h}} \sim 0.1$ from Eq. (23) where $\epsilon = \epsilon_b \sim 10^{-4}$ for our system (cf. Sect. 2.3). Such a value indicates that the vertical turbulent diffusivity is comparable with the horizontal diffusivity as a consequence of the nearly adiabatic stratification of the overshoot layer where N is very small. This conclusion does not depend strongly on the adopted value of $\nabla_{\text{ad}} - \nabla$, that is uncertain, but on the fact that the stratification is close to adiabatic.

Secondly, we assume that the turbulence produced by the tidal flow is capable of disrupting the downdrafts so that they cannot modify the stratification in the top of the radiative zone. Therefore, $\nabla_{\text{ad}} - \nabla \sim 0.04$ and $N = 5.6 \times 10^{-4} \text{ s}^{-1}$ at a depth of $0.1 H_p$ below the base of the stellar convection zone of our model of WASP-18 (cf. Sect. 3.1, Fig. 4) giving $\nu_{\text{turb v}}/\nu_{\text{turb h}} \sim 6 \times 10^{-9}$ from Eq. (23). In this regime, the turbulent diffusivity is essentially horizontal because the vertical turbulent motions are strongly hindered by the stable sub-adiabatic stratification and do not contribute in any appreciable way to the diffusivity.

In conclusion, it seems better to adopt a conservative approach and consider only the horizontal diffusivity to estimate the diffusion timescale of the downdrafts τ_d . This choice provides an upper limit for its value in the first case, while giving its order of magnitude in the second case. Specifically, we write the downdraft diffusion timescale as

$$\tau_d \sim \frac{b^2}{\nu_{\text{turb h}}}, \quad (24)$$

where b is the horizontal size of the downdrafts at the top of the overshoot layer as given by Eq. (1), while the horizontal turbulent kinematic diffusivity is given by Eq. (20).

2.8. Modifying the stratification in the overshoot layer due to tidally induced turbulence

We assume that the downdrafts are unable to significantly affect the stratification of the radiative layers below the convection zone whenever $\tau_d \ll \tau_p$, where τ_p is the characteristic lifetime of the downdrafts themselves in the absence of tides as given by Eq. (4). In other words, in this regime, the turbulent diffusivity induced by the tides strongly limits the lifetime of the downdrafts and disrupts the process leading to a nearly adiabatic stratification in the overshoot layer (Zahn 1991). On the other hand, when $\tau_d \gg \tau_p$, we assume that the downdrafts are unperturbed by the equilibrium tidal flow so they can enforce a nearly adiabatic stratification in the overshoot layer as predicted by the model by Zahn (1991).

In the intermediate regime when τ_d is comparable with τ_p , we assume that the number of downdrafts \mathcal{N} and their filling factor $f \propto \mathcal{N}$ are affected. This in turn changes the sub-adiabatic gradient because $\nabla_{\text{ad}} - \nabla$ is proportional to f according to Eq. (6). A quantification of the variation in the filling factor can be derived by considering that \mathcal{N} at any given time obeys the equation

$$\frac{d\mathcal{N}}{dt} = \frac{d\mathcal{N}_c}{dt} + \frac{d\mathcal{N}_d}{dt}, \quad (25)$$

where $d\mathcal{N}_c/dt$ is the rate of formation of new downdrafts per unit time, that we assume to be a constant k_c , while $d\mathcal{N}_d/dt$ is the rate of destruction of the downdrafts due to their intrinsic decay and the effect of the turbulent diffusion as parameterised by Eq. (24).

We may write $d\mathcal{N}_d/dt = -\mathcal{N}/\tau_0$, where τ_0 is a characteristic decay time that in the absence of any tidally induced turbulence is $\tau_0 = \tau_p$, where τ_p is the intrinsic downdraft lifetime as given by Eq. (4). On the other hand, considering a turbulent diffusion process with the timescale τ_d as given by Eq. (24) that adds its effect on the intrinsic decay of the downdraft, we find a decay of the vertical flow of the downdraft proportional to $\exp(-t/\tau_0)$, where

$$\frac{1}{\tau_0} = \frac{1}{\tau_p} + \frac{1}{\tau_d}, \quad (26)$$

as we show in Appendix A. The stationary solution of Eq. (25) gives the number of downdrafts that straddle the overshoot layer as $N = k_c \tau_0$, hence we can assume that $f \propto k_c \tau_0$. Having quantified the dependence of f on the decay timescale τ_0 of the downdrafts (see Sect. 3) we were then able to compute the impact of the additional decay produced by the tidally induced turbulence on the sub-adiabatic gradient in the overshoot layer of WASP-18 via Eq. (6).

Our analysis has been restricted to the portion of a downdraft straddling the overshoot layer assuming that the part of the same downdraft located in the overlying convection zone is not significantly perturbed by the equilibrium tidal flow. We go on to provide an argument in support of this assumption.

The oscillating equilibrium tidal flow has a period much shorter than the typical convective turnover time in the bulk of the convection zone and close to its base. Therefore, we are in the regime where the model proposed by Terquem (2023) can be applied to estimate the kinetic energy per unit mass and time exchanged between the tidal flow and an average convective downdraft. From that estimate, we derive a characteristic timescale for the kinetic energy exchange between the tidal flow and a downdraft of $\sim 2 \times 10^7$ s in the case of WASP-18, that is, one order of magnitude longer than the mean lifetime of the downdrafts as evaluated in Sect. 3.1. Therefore, we do not expect a significant influence of the tidal flow on the dynamics of the convective downdrafts in the bulk of the convection zone. The same conclusion is true for the influence of the tidal flow on a stellar dynamo working in the bulk of the convection zone because of the very small contribution of the tidal flow to the shear implying that it cannot appreciably affect the amplification, the turbulent diffusion, and the magnetic buoyancy of the magnetic field there (cf. Sect. 2.1 and the final paragraph of Appendix B).

2.9. Consequence for the storage of magnetic flux in the overshoot layer

We adopt the paradigm proposed by Moreno-Insertis et al. (1992), Ferriz-Mas & Schuessler (1994), Ferriz-Mas et al. (1994), Caligari et al. (1995, 1998), where the magnetic flux in the overshoot layer is organised into slender magnetic flux tubes that are initially stored inside the layer. Their field is steadily amplified by the radial shear of the tachocline until its intensity reaches the threshold for the onset of an undulatory instability that leads the flux tubes to emerge into the convection zone and reach the photosphere where they produce active regions.

The formation of slender magnetic flux tubes from an initial nearly uniform layer of magnetic azimuthal flux can be a consequence of the penetrative convection and of magnetic field instabilities as discussed, for instance, by Fan (2021). Although some difficulties have been put forward for the operation of such a paradigm in the solar and stellar convection zones and overshoot layers (cf. Sect. 11 in Fan 2021; Hughes 2007), we consider such a model in view of its simplicity, in particular the possibility of analytically predicting the instability of the slender magnetic flux tubes in the overshoot layer thanks to the approach introduced by Ferriz-Mas & Schuessler (1994). It is interesting to note that the storage and emergence of flux tubes from the overshoot layer of the Sun have recently been modelled by Manek et al. (2022) to account for the observed hemispheric dependence of the sign of magnetic helicity in solar active regions, thus providing further support to our assumptions about the key role of the overshoot layer in stellar activity.

When the downdrafts are allowed to establish a nearly adiabatic stratification in the overshoot layer, the sub-adiabatic gra-

dient is such that $\nabla_{\text{ad}} - \nabla \sim (0.1 - 1) \times 10^{-5}$. In this regime, the slender magnetic flux tubes stored and amplified within the layer become unstable with a growth timescale of the order of one year for a field intensity of ~ 10 T (cf. Ferriz-Mas & Schuessler 1994) and, after penetrating in the overlying convection zone, emerge almost radially forming active regions at low latitudes in the stellar photosphere (Caligari et al. 1995; Granzer et al. 2000). On the other hand, when the convective downdrafts are made ineffective by the turbulent diffusivity due to tides, the stratification in the former overshoot layer becomes that of the radiative interior with a much larger sub-adiabatic gradient difference $\nabla_{\text{ad}} - \nabla \sim 0.04$ (see Sect. 3.1, Fig. 4). This implies that a field intensity much larger than 10 T is required to produce the flux tube instability, that we assume to be impossible to attain for the stellar dynamo because it is quenched by the magnetic field itself (cf. Moreno-Insertis et al. 1995; Gilman & Rempel 2005). As a consequence, the slender flux tubes remain stably stored inside the overshoot layer and cannot emerge to form active regions in the photosphere.

In the intermediate regime when $\tau_p \sim \tau_d$, we have a decrease in the filling factor, f , of the downdrafts because we know that $f \propto k_c \tau_0$ (Sect. 2.8). As a consequence, the gradient becomes more sub-adiabatic, that is, the difference $\nabla_{\text{ad}} - \nabla$ increases because it is inversely proportional to f (cf. Eq. 6). Therefore, the undulatory instability of the slender flux tubes stored in the overshoot layer is hampered because it requires a remarkably stronger field to develop. For example, looking at Fig. 8 of Ferriz-Mas & Schuessler (1994), we see that the threshold for the development of the instability is at a field intensity of 13.5 T when $\nabla_{\text{ad}} - \nabla = 10^{-6}$ in the Sun, while it increases to 15 T when $\nabla_{\text{ad}} - \nabla = 2 \times 10^{-6}$ that corresponds to a decrease in f by a factor of 2 that is obtained when $\tau_p \sim \tau_d$. Such a stronger magnetic field intensity may not be reachable through the dynamo amplification leading to the same situation described above in the case of the downdraft disruption. In other words, the magnetic flux tubes may not be capable of developing the instability that allows them to emerge to the photosphere. This will strongly reduce the level of stellar activity. As we show in the next section (Sect. 3), this could be the case in WASP-18, thus providing a possible explanation for its depressed activity level.

The above conclusion is based on the assumed filamentary structure of the toroidal field in the overshoot layer. If the field is structured as a continuous layer rather than as discrete individual slender flux tubes, it is important to take into account other kinds of instabilities that are specific to such a layer. Previously, we pointed out that the magnetic pumping by the downdrafts should lead to the formation of such a layer and confine it to the lower part of the overshoot region. Therefore, we present an analysis of the relevant instabilities in a continuous magnetic layer in Appendix B. It confirms the conclusion we reached by means of the slender flux tube model, that is, also a continuous magnetic layer is stabilised by an increase in the sub-adiabatic gradient in the overshoot region below the convection zone.

3. Application to the WASP-18 system

In order to make a quantitative application of the model proposed above to the WASP-18 system, we need a model of the star internal structure that is described in the next Sect. 3.1. Using that model, we compute estimates for the turbulent diffusivity and study the regime occurring in the stellar overshoot layer and its possible consequences on stellar activity in Sect. 3.2.

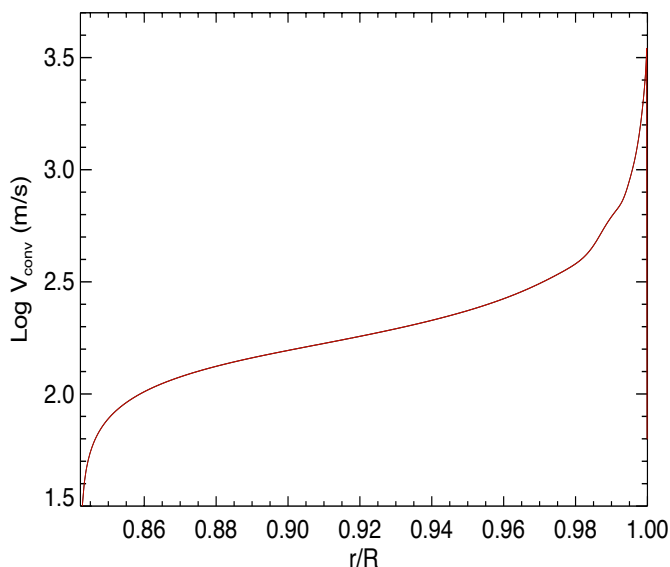


Fig. 2. Logarithm of the convective velocity V_{conv} vs. the stellar radius r in units of the photospheric radius R in the outer convection zone of our interior model (red solid line).

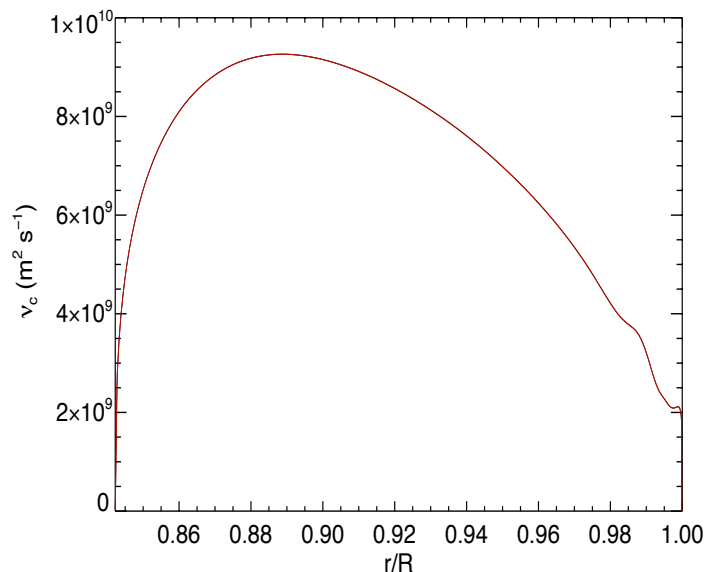


Fig. 3. Turbulent convective diffusivity ν_c vs. the stellar radius r in units of the photospheric radius R as derived from our stellar interior model (red solid line).

3.1. Stellar interior model

A stellar interior and evolution model has been computed by means of the Modules for Experiments in Stellar Astrophysics (MESA) code (Paxton et al. 2019, and references therein) that has been run through the web interface MESA-Web². The model has been computed for a non-rotating star of initial mass of $1.22 M_{\odot}$ and a solar metallicity ($Z = 0.02$) with the basic network for nuclear reactions; the mixing-length parameter $\alpha_{\text{mlt}} = 2.0$, while the overshooting parameters were assumed to be very small ($f = 10^{-4}$ and $f_0 = 5 \times 10^{-4}$; these parameters control the length scale of the exponential decay of the diffusive overshooting and the lower boundary of the overshoot region, respectively, and are not to be confused with the downdraft filling factor f considered in the present work; see Moravveji et al. 2016, Sect. 3, for their definition). We note that such overshooting parameters have an impact on the internal diffusion mainly during late evolutionary phases of the stellar model (cf. Sect. 5.2 of Paxton et al. 2011), so they do not affect our application for which we may assume an internal structure model computed without a significant overshooting at the base of the outer convection zone. We selected the interior structure model corresponding to an age of 662.5 Myr, when the star has a radius $R = 1.208 R_{\odot}$ that matches closely the radius of WASP-18 ($R = 1.216 \pm 0.067 R_{\odot}$; Hellier et al. 2009). The base of the convection zone determined according to the Schwarzschild criterion is at $r_b/R = 0.8438$ and the convective velocity in that layer is 45.9 m s^{-1} ; the pressure scale height there is $H_p = 4.376 \times 10^7 \text{ m}$, the density $\rho_b = 10.4 \text{ kg m}^{-3}$, and the temperature 1.054 MK .

In Fig. 2, we plot the convective velocity V_{conv} as computed from the mixing-length theory vs. the radius in the convection zone of our interior model. The rapid decrease in the density towards the photosphere makes the convective velocity increase remarkably in order to transport the whole stellar luminosity that

amounts to $2.0 L_{\odot}$ in our model. The convective turnover time at the base of the convection zone, that is adopted as the downdraft lifetime in our model, is $\tau_p \sim 1.8 \times 10^6 \text{ s}$ or ~ 21 days by applying Eq. (4). On the other hand, the asteroseismic calibration by Corsaro et al. (2021), indicates an average convective turnover time of $\sim 29 \pm 8$ days for a MS star with $B-V = 0.49$, the colour index of WASP-18. Therefore, our estimate of the convective turnover time at the base of the convection zone, and consequently of τ_p , should likely be regarded as a lower limit for our star.

In Fig. 3, we plot the convective turbulent diffusivity $\nu_c \sim \alpha_{\text{mlt}} H_p(r) V_{\text{conv}}(r)$ vs. the stellar radius r . It is useful for a comparison with the diffusivity produced by the turbulence induced by the tidal flow according to our mechanism (see Sect. 3.2). The value of ν_c averaged over the whole volume of the convection zone is $\bar{\nu}_c \sim 7.0 \times 10^9 \text{ m}^2 \text{ s}^{-1}$.

In Fig. 4, we plot the difference between the adiabatic and the actual stellar thermal gradient $\delta \equiv \nabla_{\text{ad}} - \nabla$ vs. the stellar radius close to and below the base of our model convection zone. The base of the stellar convection zone according to the Schwarzschild criterion is indicated by the right vertical green dashed line where $\delta = 0$, while the left green vertical dashed line is drawn below a depth of $0.1 H_p$ from the base of the convection zone, where H_p is the pressure scale height at the base of the convection zone. Such a depth is assumed to be the vertical extension of the overshoot layer, L_p , that is, the penetration depth of the convective downdrafts. The difference between the adiabatic gradient and the actual temperature gradient increases rapidly as one moves into the radiative interior because our model has been computed without a significant amount of overshooting, thus it does not include the effects of the downdrafts on the thermal stratification.

The depth, z_0 , of the convection zone in our model of WASP-18 is 0.156 stellar radii or $1.31 \times 10^8 \text{ m}$. The corresponding radius of the convective downdrafts at the base of the convection zone, computed by means of Eq. (1), is $b = 6.6 \times 10^6 \text{ m}$, while the ini-

² <http://user.astro.wisc.edu/~townsend/static.php?ref=mesa-web>

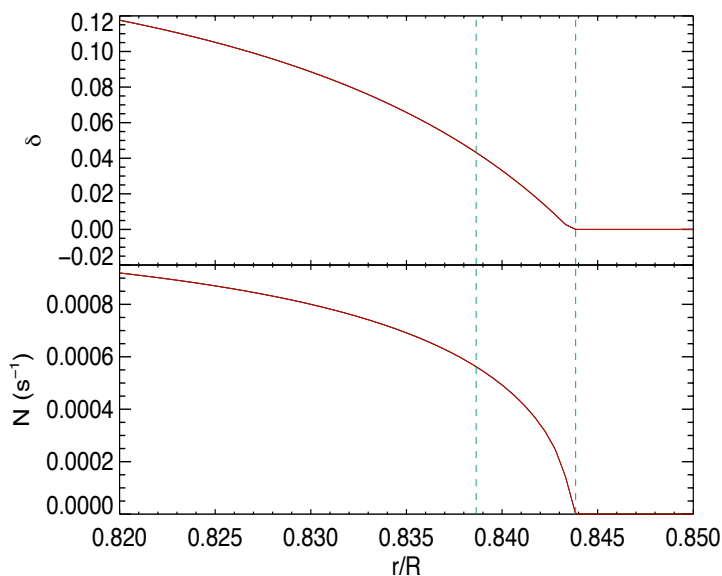


Fig. 4. Difference of $\delta = \nabla_{\text{ad}} - \nabla$ between the adiabatic thermal gradient and the actual stellar thermal gradient (upper panel) and the Brunt-Väisälä frequency N (lower panel) vs. the stellar radius r in units of the photospheric radius R (red solid lines). The vertical green dashed lines bound a layer of thickness $L_p = 0.1 H_p$, where H_p is the pressure scale height at the base of the stellar convection zone.

tial velocity of penetration $V_b = 453 \text{ m s}^{-1}$ according to Eq. (2). A plot of the penetration velocity vs. the depth expressed as a fraction of the penetration depth, L_p , is shown in Fig. 5 and has been computed by means of Eq. (3). We note the fast braking of the plumes as they approach the penetration depth L_p where there is a thin boundary layer separating the overshoot layer from the radiative zone below (see Sect. 3.2 of Zahn 1991, for details).

Our interior model together with the above estimate of the initial velocity of the downdrafts can be used to evaluate the deviation of the stratification from the adiabatic gradient in the overshoot layer by means of Eq. (6), giving $\nabla_{\text{ad}} - \nabla \sim 6.5 \times 10^{-6}$ for a plume filling factor $f = 0.1$. This result shows that the downdrafts are very efficient in bringing the stratification very close to a perfectly adiabatic one. The gradient, however, remains slightly sub-adiabatic, that is crucial to allow the storage of magnetic flux tubes and set the threshold for their instability (cf. Ferriz-Mas & Schuessler 1994).

3.2. Turbulence in the overshoot layer and its effects on the downdrafts and stratification

As we show in Sect. 2.3, the close-by and massive planet WASP-18b produces a tidal deformation of $\epsilon_b \sim 1.0 \times 10^{-4}$ and a horizontal tidal velocity of $\sim 18 \text{ m s}^{-1}$ in the overshoot layer. Applying Eq. (20) with $\omega_{\text{tide}} = 1.3 \times 10^{-4} \text{ s}^{-1}$, we find a horizontal turbulent diffusivity in that layer of $\nu_{\text{turbh}} \sim 4 \times 10^8 \text{ m}^2 \text{ s}^{-1}$. The diffusion timescale of a downdraft of size $b = 6.6 \times 10^6 \text{ m}$ is of $\tau_d \sim 1.1 \times 10^5 \text{ s}$ according to Eq. (4), that is, a factor of ~ 16 shorter than the downdraft lifetime τ_p as estimated from our interior model and Eq. (24). Adopting the average convective turnover time estimated with the calibration by Corsaro et al. (2021) as the downdraft lifetime, we obtain a ratio $\tau_p/\tau_d \sim 23 \pm 7$.

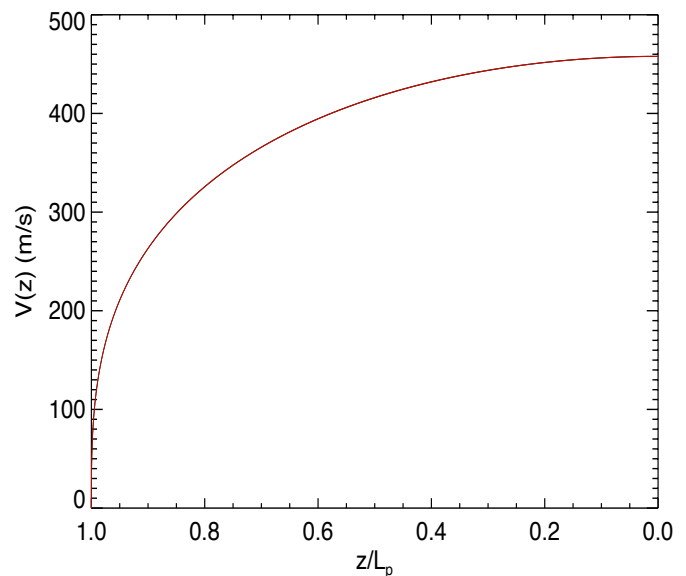


Fig. 5. Velocity of the downdrafts in the overshoot layer of our model vs. the depth z below the base of the convection zone measured in units of L_p , that is, the penetration of the plumes below the standard convection zone.

According to the simple model introduced in Sect. 2.8, we have a value of τ_0 that is reduced by a factor of ~ 25 with respect to the case without equilibrium tide. The corresponding filling factor f of the downdrafts that appears in Eq. (6) is therefore reduced by the same factor that implies an increase in the sub-adiabaticity $\nabla_{\text{ad}} - \nabla$ by a factor of ~ 25 , that is, from $\nabla_{\text{ad}} - \nabla \sim 6.5 \times 10^{-6}$ (cf. Sect. 3.1) to $\nabla_{\text{ad}} - \nabla \sim 1.6 \times 10^{-4}$. As a consequence, the slender magnetic flux tubes stored in the overshoot layer must reach a remarkably larger field strength to become unstable and emerge to the stellar photosphere.

In Fig. 6, we show the stability diagram of such flux tubes computed by means of Eq. (40) of Ferriz-Mas & Schuessler (1994) for the most unstable mode with azimuthal wavenumber $m = 1$. The radial differential rotation parameter $q = 0.06$, that is, similar to the solar value, while the difference between the angular velocity of the plasma outside and inside the flux tube is assumed to be maximal, that is, equal to v_A/r_b , where v_A is the Alfvén velocity inside the flux tube (see Ferriz-Mas & Schuessler 1994, for the definition and role of these parameters). We consider two values of the sub-adiabatic gradient, that is, $\nabla_{\text{ad}} - \nabla = 6.5 \times 10^{-6}$, that corresponds to the stratification in the overshoot layer of WASP-18 without the perturbation due to the tides, and $\nabla_{\text{ad}} - \nabla = 1.6 \times 10^{-4}$, that corresponds to the increased sub-adiabaticity produced by the reduced efficiency of the downdrafts under the action of the equilibrium tide. As can be seen from Fig. 6, the threshold field for the instability of the flux tubes in the overshoot layer of WASP-18 increases from $\sim 11.5 \text{ T}$ to 16.5 T when we consider the effect of the tidal flow on the downdrafts. This corresponds to an increase in the magnetic energy density by a factor of ~ 2 . If the stellar hydro-magnetic dynamo is unable to produce a field strength that exceeds such an increased instability threshold, the magnetic flux tubes stored in the stellar overshoot layer cannot emerge and the magnetic activity of WASP-18 is depressed providing a possible explanation for the observations.

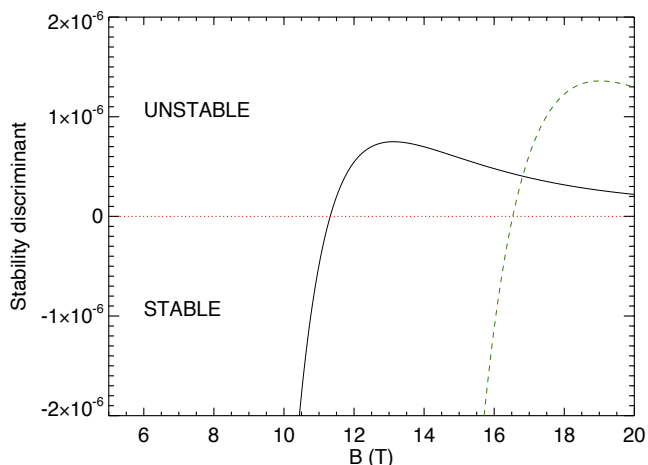


Fig. 6. Stability diagram of a slender flux tube to the $m = 1$ mode computed according to Ferriz-Mas & Schuessler (1994) for two different values of the sub-adiabatic gradient in the overshoot layer $\nabla_{\text{ad}} - \nabla = 6.5 \times 10^{-6}$ (black solid line) and 1.6×10^{-4} (green dashed line). The horizontal red dotted line marks the transition from a stable to an unstable flux tube (see text).

We could consider a slow inflow of heat due to radiative conductivity, bringing a flux tube into thermal equilibrium with its surroundings, as a possible way of reducing flux tube stability because a flux tube in thermal equilibrium would become buoyantly unstable. However, the timescale for such a mechanism to operate is of the order of L_p^2/K , assuming the flux tubes have a diameter comparable with the vertical extension of the overshoot layer. From our model we find, $L_p \sim 4.4 \times 10^6$ m and $K \sim 3.9 \times 10^4$ m² s⁻¹ that gives a thermal diffusion time of the order of ~ 15 years, that is, remarkably longer than the typical short stellar activity cycles observed in rapidly rotating F-type stars having a length of $\sim 0.3 - 3$ years (cf. Mittag et al. 2019). Therefore, we rule out such a mechanism as a source of flux tube destabilisation because it cannot operate over timescales shorter than the stellar cycles as required to account for the activity of such stars.

Finally, in Appendix B, we consider the case when the magnetic flux in the overshoot region is organised as a continuous magnetic layer. We find that an increase in the sub-adiabatic stratification leads to a remarkably larger threshold for the field instability also in that case, notably also considering the doubly diffusive instability or the overstability that are not included in the model by Ferriz-Mas & Schuessler (1994). Therefore, the above conjecture about the suppression of magnetic activity in WASP-18 by the action of the equilibrium tide is not critically dependent on our assumption on the field organisation in the overshoot layer.

3.3. The case of a more distant or lighter planet

WASP-18b was probably formed at a larger distance than the present separation where it was likely brought by the tides it raised on the star (e.g. Collier Cameron & Jardine 2018). Considering a past separation of twice the present value, the deformation parameter ϵ becomes 8 times smaller and the tidal frequency about 2.8 times smaller leading to an horizontal tidal velo-

city of only 0.8 m s⁻¹ and a turbulent horizontal diffusivity as estimated from Eq. (20) of $\nu_{\text{turb h}} \sim 4 \times 10^6$ m² s⁻¹ (cf. the dependence of $\nu_{\text{turb h}}$ on $(\omega_{\text{tide}} \epsilon_b)^{3/2}$ in Eq. 20). The diffusion timescale of the downdrafts becomes $\tau_d \sim 1.1 \times 10^7$ s, that is, about a factor of $\sim 4 - 5$ times longer than the typical downdraft lifetime. Therefore, a modest modification is expected to occur in the overshoot layer stratification as a consequence of the equilibrium tide raised by the planet. We conclude that WASP-18 has been caught in a particular phase of its evolution when the proximity and the large mass of its planet can modify the stratification in its overshoot layer, possibly hampering its magnetic activity.

Similar conclusions apply if we consider a planet of lower mass on the same close-by orbit. For example, in the case of WASP-12, the hot Jupiter has a mass of 1.36 Jupiter masses and an orbital separation of 0.023 au comparable with that of WASP-18b. In that system, we expect an increase in the diffusion time by a factor of ~ 30 with respect to WASP-18 because of the dependence on $\epsilon_b^{3/2}$ of the turbulent diffusivity. Therefore, the decrease in τ_0 and consequently in f is only by a factor of ~ 2 , that should not produce a significant effect on the flux tube stability and stellar activity. In conclusion, the apparent depressed chromospheric activity of WASP-12 should be interpreted in the framework of a circumstellar absorption model, as mentioned in Sect. 1.

4. Discussion and conclusions

We propose a conjectural model to account for the very low level of magnetic activity observed in WASP-18 based on the disruption of the convective plumes in its overshoot layer and the consequent hindering of the process of starspot formation in its photosphere. Such a disruption is a consequence of the interaction of the horizontal tidal flow with the vertical obstacles represented by the convective downdrafts in the overshoot layer that leads to an enhanced turbulent diffusion with respect to the case of a star without tidal interactions.

We have presented plausibility arguments to support the hypotheses upon which our model is based. Admittedly, most of them rely on simplified analytical models of physical processes that are very difficult or impossible to simulate numerically in the regimes characteristic of stellar interiors. Therefore, our proposal must be regarded as speculative and is presented in order to stimulate further observational and theoretical investigations on the effects of close-by massive planets on stellar magnetic activity.

The mechanism proposed in this paper can work only in a restricted range of mass and separation of the close-by planet, while a basic requirement for its operation is a large tidal frequency, ω_{tide} , which is possible only if the stellar host is not synchronised. Therefore, our mechanism cannot operate in close stellar binary systems because both their components are synchronised. In the case of WASP-18, our model suggests that the inhibition of stellar activity has begun only rather recently in the evolution of the system because the invoked effect was not relevant when the separation of the planet was twice the present one. The timescale for the orbital decay of the system depends on the ill-known modified tidal quality factor of the star that can be as large as $Q'_{\text{star}} \gtrsim 2 \times 10^8$ in a system away from synchronisation as WASP-18 leading to a remaining lifetime before engulfment of the order of 100 Myr, despite the very close orbit of the planet (cf. Ogilvie & Lin 2007; Mathis 2015; Bonomo et al. 2017; Collier Cameron & Jardine 2018).

The additional turbulent dissipation invoked in our model has a negligible effect on the dissipation of the equilibrium (and pos-

sibly dynamical) tide because it is smaller by a factor of $\sim 15\text{--}20$ than the average turbulent diffusivity $\bar{\nu}_c$ due to the convective motions in the stellar convection zone (cf. Sect. 3.1) that are regarded as the main source of dissipation of the equilibrium tide (Zahn 1977)³. Moreover, it is limited to the shallow overshoot layer, while the turbulent dissipation of the equilibrium tide occurs over the whole convection zone.

Other possible observational consequences of the mechanism proposed in this work concern the excitation of gravity waves in the stellar radiative zone (Breton et al. 2022) and the process leading to the inward diffusion and nuclear burning of light elements (Montalbán & Schatzman 2000). These aspects merit a dedicated investigation in future works since we have qualitatively predicted a current lower efficiency for both such processes in WASP-18, given the disruption of the downdrafts in the overshoot layer of this star.

Acknowledgements. The authors are grateful to Dr. S. Mathis for useful discussions and suggestions. They acknowledge the careful and critical reading by an anonymous Referee that significantly helped to improve the original version of this work. AFL acknowledges support from INAF through their program entitled "Unveiling the magnetic side of the stars" (P.I. Dr. A. Bonanno) financed by a theory grant approved as part of the INAF initiative to foster Fundamental Astrophysics.

References

- Alvan, L., Brun, A. S., & Mathis, S. 2014, A&A, 565, A42. doi:10.1051/0004-6361/201323253
- Anders, E. H., Jermyn, A. S., Lecoanet, D., et al. 2022, ApJ, 926, 169. doi:10.3847/1538-4357/ac408d
- Baraffe, I., Pratt, J., Vlaykov, D. G., et al. 2021, A&A, 654, A126. doi:10.1051/0004-6361/202140441
- Baraffe, I., Clarke, J., Morison, A., et al. 2023, MNRAS, 519, 5333. doi:10.1093/mnras/stad009
- Barekat, A., Schou, J., & Gizon, L. 2014, A&A, 570, L12. doi:10.1051/0004-6361/201424839
- Barker, A. J. 2020, MNRAS, 498, 2270. doi:10.1093/mnras/staa2405
- Barnabé, R., Strugarek, A., Charbonneau, P., et al. 2017, A&A, 601, A47. doi:10.1051/0004-6361/201630178
- Baum, A. C., Wright, J. T., Luhn, J. K., et al. 2022, AJ, 163, 183. doi:10.3847/1538-3881/ac5683
- Bearman, P. W. 1984, Annual Review of Fluid Mechanics, 16, 195. doi:10.1146/annurev.fl.16.010184.001211
- Biswas, A., Karak, B. B., Usoskin, I., et al. 2023, Space Sci. Rev., 219, 19. doi:10.1007/s11214-023-00968-w
- Böhm-Vitense, E. 2007, ApJ, 657, 486. doi:10.1086/510482
- Bonomo, A. S., Desidera, S., Benatti, S., et al. 2017, A&A, 602, A107. doi:10.1051/0004-6361/201629882
- Brandenburg, A., Mathur, S., & Metcalfe, T. S. 2017, ApJ, 845, 79. doi:10.3847/1538-4357/aa7cfa
- Brandenburg, A., Elstner, D., Masada, Y., et al. 2023, Space Sci. Rev., 219, 55. doi:10.1007/s11214-023-00999-3
- Breton, S. N., Brun, A. S., & García, R. A. 2022, A&A, 667, A43. doi:10.1051/0004-6361/202244247
- Brun, A. S. & Browning, M. K. 2017, Living Reviews in Solar Physics, 14, 4. doi:10.1007/s41116-017-0007-8
- Brun, A. S., Strugarek, A., Varela, J., et al. 2017, ApJ, 836, 192. doi:10.3847/1538-4357/aa5c40
- Brun, A. S. & Zahn, J.-P. 2006, A&A, 457, 665. doi:10.1051/0004-6361:20053908
- Caligari, P., Moreno-Insertis, F., & Schuessler, M. 1995, ApJ, 441, 886. doi:10.1086/175410
- Caligari, P., Schüssler, M., & Moreno-Insertis, F. 1998, ApJ, 502, 481. doi:10.1086/305875
- Charbonneau, P. 2020, Living Reviews in Solar Physics, 17, 4. doi:10.1007/s41116-020-00025-6
- Cloutier, S., Cameron, R. H., & Gizon, L. 2023, A&A, 680, A42. doi:10.1051/0004-6361/202347022
- Collier Cameron, A. & Jardine, M. 2018, MNRAS, 476, 2542. doi:10.1093/mnras/sty292
- Corsaro, E., Bonanno, A., Mathur, S., et al. 2021, A&A, 652, L2. doi:10.1051/0004-6361/202141395
- Dandoy, V., Park, J., Augustson, K., et al. 2023, A&A, 673, A6. doi:10.1051/0004-6361/202243586
- Fan, Y. 2021, Living Reviews in Solar Physics, 18, 5. doi:10.1007/s41116-021-00031-2
- Ferriz-Mas, A. & Schuessler, M. 1994, ApJ, 433, 852. doi:10.1086/174694
- Ferriz-Mas, A., Schmitt, D., & Schuessler, M. 1994, A&A, 289, 949
- Fossati, L., Ayres, T. R., Haswell, C. A., et al. 2013, ApJ, 766, L20. doi:10.1088/2041-8205/766/2/L20
- Fossati, L., Ingrassia, S., & Lanza, A. F. 2015, ApJ, 812, L35. doi:10.1088/2041-8205/812/2/L35
- Fossati, L., Koskinen, T., France, K., et al. 2018, AJ, 155, 113. doi:10.3847/1538-3881/aaa891
- Gilman, P. A. & Rempel, M. 2005, ApJ, 630, 615. doi:10.1086/431929
- Granzer, T., Schüssler, M., Caligari, P., et al. 2000, A&A, 355, 1087
- Guerrero, G., Smolarkiewicz, P. K., de Gouveia Dal Pino, E. M., et al. 2016, ApJ, 819, 104. doi:10.3847/0004-637X/819/2/104
- Haswell, C. A., Fossati, L., Ayres, T., et al. 2012, ApJ, 760, 79. doi:10.1088/0004-637X/760/1/79
- Hellier, C., Anderson, D. R., Collier Cameron, A., et al. 2009, Nature, 460, 1098. doi:10.1038/nature08245
- Hughes, D. W. 2007, in The Solar Tachocline, D. W. Hughes, R. Rosner, & N. O. Weiss (Eds.), Cambridge Univ. Press, Cambridge, pp. 275-298
- Hughes, D. W. & Brummell, N. H. 2021, ApJ, 922, 195. doi:10.3847/1538-4357/ac2057
- Isaacson, H., Kane, S. R., Carter, B., et al. 2024, ApJ, 961, 85. doi:10.3847/1538-4357/ad077b
- Käpylä, P. J., Rheinhardt, M., Brandenburg, A., et al. 2020, A&A, 636, A93. doi:10.1051/0004-6361/201935012
- Käpylä, P. J., Browning, M. K., Brun, A. S., et al. 2023, Space Sci. Rev., 219, 58. doi:10.1007/s11214-023-01005-6
- Karak, B. B. 2023, Living Reviews in Solar Physics, 20, 3. doi:10.1007/s41116-023-00037-y
- Khodkar, M. A., Klamo, J. T., and Kunihiko Taira, K. 2021, Phys. Rev. Fluids 6, 034401, doi: 10.1103/PhysRevFluids.6.034401
- Kippenhahn, R., Weigert, A., & Weiss, A. 2013, Stellar Structure and Evolution. ISBN: 978-3-642-30304-3. Berlin, Heidelberg: Springer Berlin Heidelberg, 2013.. doi:10.1007/978-3-642-30304-3
- Kitchatinov, L. L., Pipin, V. V., & Ruediger, G. 1994, Astronomische Nachrichten, 315, 157. doi:10.1002/asna.2103150205
- Kitchatinov, L. L. & Brandenburg, A. 2012, Astronomische Nachrichten, 333, 230. doi:10.1002/asna.201211648
- Korre, L. & Featherstone, N. A. 2021, ApJ, 923, 52. doi:10.3847/1538-4357/ac2dea
- Lanza, A. F. 2014, A&A, 572, L6. doi:10.1051/0004-6361/201425051
- Lecoanet, D. & Quataert, E. 2013, MNRAS, 430, 2363. doi:10.1093/mnras/stt055
- Manek, B., Pontin, C., & Brummell, N. 2022, ApJ, 929, 162. doi:10.3847/1538-4357/ac5828
- Mathis, S. 2015, A&A, 580, L3. doi:10.1051/0004-6361/201526472
- Mathis, S., Prat, V., Amard, L., et al. 2018, A&A, 620, A22. doi:10.1051/0004-6361/201629187
- Mittag, M., Schmitt, J. H. M. M., Hempelmann, A., et al. 2019, A&A, 621, A136. doi:10.1051/0004-6361/201834319
- Montalbán, J. & Schatzman, E. 2000, A&A, 354, 943
- Moravvejii, E., Townsend, R. H. D., Aerts, C., et al. 2016, ApJ, 823, 130. doi:10.3847/0004-637X/823/2/130
- Moreno-Insertis, F., Schuessler, M., & Ferriz-Mas, A. 1992, A&A, 264, 686
- Moreno-Insertis, F., Caligari, P., & Schuessler, M. 1995, ApJ, 452, 894. doi:10.1086/176357
- Nazarenko, S. 2011, Wave Turbulence, Lecture Notes in Physics, vol. 825, Berlin: Springer, 2011. ISBN: 978-3-642-15941-1
- Ogilvie, G. I. 2014, ARA&A, 52, 171. doi:10.1146/annurev-astro-081913-035941
- Ogilvie, G. I. & Lin, D. N. C. 2007, ApJ, 661, 1180. doi:10.1086/515435
- Paxton, B., Bildsten, L., Dotter, A., et al. 2011, ApJS, 192, 3. doi:10.1088/0067-0049/192/1/3
- Paxton, B., Smolec, R., Schwab, J., et al. 2019, ApJS, 243, 10. doi:10.3847/1538-4365/ab2241
- Pillitteri, I., Wolk, S. J., Sciortino, S., et al. 2014, A&A, 567, A128. doi:10.1051/0004-6361/201423579
- Pillitteri, I., Colombo, S., Micela, G., et al. 2023, A&A, 673, A61. doi:10.1051/0004-6361/202245467

- Pinçon, C., Belkacem, K., & Goupil, M. J. 2016, *A&A*, 588, A122.
doi:10.1051/0004-6361/201527663
- Pinçon, C., Appourchaux, T., & Buldgen, G. 2021, *A&A*, 650, A47.
doi:10.1051/0004-6361/202040003
- Pipin, V. V. & Kosovichev, A. G. 2011, *ApJ*, 727, L45. doi:10.1088/2041-8205/727/2/L45
- Pratt, J., Baraffe, I., Goffrey, T., et al. 2017, *A&A*, 604, A125. doi:10.1051/0004-6361/201630362
- Priest, E. R. 1984, *Solar Magnetohydrodynamics*, Geophysics and Astrophysics Monographs, D. Reidel Publ. Co., Dordrecht: Reidel, 1984
- Remus, F., Mathis, S., & Zahn, J.-P. 2012, *A&A*, 544, A132. doi:10.1051/0004-6361/201118160
- Ricker, G. R., Winn, J. N., Vanderspek, R., et al. 2015, *Journal of Astronomical Telescopes, Instruments, and Systems*, 1, 014003. doi:10.1117/1.JATIS.1.1.014003
- Rieutord, M. & Zahn, J.-P. 1995, *A&A*, 296, 127
- Schmitt, J. H. M. M. & Rosner, R. 1983, *ApJ*, 265, 901. doi:10.1086/160734
- Schou, J., Antia, H. M., Basu, S., et al. 1998, *ApJ*, 505, 390. doi:10.1086/306146
- Seguin, F. H. 1976, *ApJ*, 207, 848. doi:10.1086/154555
- Solanki, S. K. 2003, *A&A Rev.*, 11, 153. doi:10.1007/s00159-003-0018-4
- Spiegel, E. A. & Zahn, J.-P. 1992, *A&A*, 265, 106
- Strugarek, A., Brun, A. S., & Zahn, J.-P. 2011, *A&A*, 532, A34. doi:10.1051/0004-6361/201116518
- Terquem, C. 2023, *MNRAS*, 525, 508. doi:10.1093/mnras/stad2163
- Tobias, S. M., Brummell, N. H., Clune, T. L., et al. 1998, *ApJ*, 502, L177. doi:10.1086/311501
- Tobias, S. M., Brummell, N. H., Clune, T. L., et al. 2001, *ApJ*, 549, 1183. doi:10.1086/319448
- Vidal, J., Cébron, D., ud-Doula, A., et al. 2019, *A&A*, 629, A142. doi:10.1051/0004-6361/201935658
- Weinberg, N. N., Arras, P., Quataert, E., et al. 2012, *ApJ*, 751, 136. doi:10.1088/0004-637X/751/2/136
- Williamson, C. H. K. 1996, *Annual Review of Fluid Mechanics*, 28, 477. doi:10.1146/annurev.fl.28.010196.002401
- Zahn, J.-P. 1977, *A&A*, 57, 383
- Zahn, J.-P. 1991, *A&A*, 252, 179
- Zahn, J.-P., Talon, S., & Matias, J. 1997, *A&A*, 322, 320. doi:10.48550/arXiv.astro-ph/9611189
- Zdravkovich, M. M. 1997, *Flow Around Circular Cylinders*, Cambridge Univ. Press, Cambridge,

Appendix A: Downdraft diffusion under the action of turbulent diffusivity

In the presence of turbulent diffusivity in the overshoot layer as we expect to be produced by the equilibrium tidal flow, the lifetime of the downdrafts is affected and their decay is faster than their intrinsic timescale τ_p as set by the convective flow.

In order to estimate the effect of the turbulent diffusivity, we assume that the decay of the velocity field of the downdraft is ruled by a diffusion equation to which we add the contribution due to the intrinsic decay of the convective flow, that is,

$$\frac{\partial v}{\partial t} = v_{\text{turbh}} \nabla_{\text{h}}^2 v - \frac{v}{\tau_p}, \quad (\text{A.1})$$

where we consider only the effect of the horizontal turbulent diffusivity as parameterised by v_{turbh} because the turbulent vertical diffusivity is hampered by the sub-adiabatic stratification in the overshoot layer of WASP-18 (cf. Sect. 2.7). Considering that the downdraft is symmetric around its vertical axis (cf. Rieutord & Zahn 1995), the horizontal Laplacian is given by:

$$\nabla_{\text{h}}^2 = \frac{1}{s} \frac{\partial}{\partial s} \left(s \frac{\partial}{\partial s} \right). \quad (\text{A.2})$$

We look for a solution of Eq. (A.1) of the form:

$$v = g(t) v_{\text{down}}(s, z, t), \quad (\text{A.3})$$

where $g(t)$ is a function of the time that accounts for the effect of the turbulent diffusivity only and v_{down} is the downdraft velocity field in the absence of diffusivity as given by Eq. (5).

Rigorously speaking, a solution of the form presented in Eq. (A.3) is not allowed in the case of Eq. (A.1), except along the axis of symmetry of the downdraft, that is, for $s = 0$, as can be immediately verified by substituting the trial solution from Eq. (A.3) into the same equation. Therefore, limiting ourselves to a solution along the axis $s = 0$, we substitute Eq. (A.3) into Eq. (A.1). Thus, we obtain:

$$\frac{dg}{dt} = - \left(\frac{2v_{\text{turbh}}}{b^2} \right) g(t), \quad (\text{A.4})$$

which gives

$$g(t) = \exp \left(- \frac{t}{\tau_d} \right), \quad (\text{A.5})$$

where $\tau_d = b^2 / (2v_{\text{turbh}})$ is the turbulent diffusion timescale. Given that our model provides only an order-of-magnitude estimate, we adopt the turbulent diffusion time τ_d as given by Eq. (24). When we combine the intrinsic decay of the downdraft with the timescale τ_p (cf. Eq. 5) with the additional turbulent decay as given by the solution (A.5), we obtain a time dependence of its flow proportional to $\exp(-t/\tau_d) \exp(-t/\tau_p)$, that gives the expression for the lifetime of the downdraft in Eq. (26).

Appendix B: Instabilities in a continuous magnetic layer

Our approach assuming that the magnetic field in the overshoot layer is organised as a set of discrete slender flux tubes has the advantage of a great simplification in the treatment of the effects of field curvature, external stratification, and differential rotation,

but it cannot include important physical effects such as the doubly diffusive instability that can destabilise a continuous magnetic layer, even in the presence of a strong sub-adiabatic stratification (Schmitt & Rosner 1983; Hughes & Brummell 2021). A discussion of this effect is provided by Hughes (2007), for instance, and we follow this approach in view of their simplicity and focusing on the basic physics. Neglecting the effect of rotation and assuming that there is no bending of the magnetic field lines, the criterion for the onset of the doubly diffusive instability is:

$$- \frac{gV_A^2}{c_s^2} \frac{d}{dz'} \ln B > \frac{\eta}{\kappa} N^2, \quad (\text{B.1})$$

where V_A is the Alfvén velocity, c_s the sound speed, g the acceleration of gravity, z' the vertical coordinate increasing toward the stellar surface, η the magnetic diffusivity, κ the thermal conductivity, and N the Brunt-Väisälä frequency. In the radiative zone of a star, $\eta \ll \kappa$; therefore, a small perturbation of the magnetic field can exchange heat and reach the temperature of its surrounding, while its magnetic field diffuses much more slowly. This maintains the unstable field gradient responsible for the growth of the perturbation and keeps the field buoyant during its motion, thus increasing the amplitude of the initial perturbation. Given that the ratio of the microscopic diffusivities $\eta/\kappa \sim 10^{-4}$ in the upper radiative zone of the Sun (Brun & Zahn 2006), even a strongly stable stratification, corresponding to a large value of the Brunt-Väisälä frequency N , cannot prevent the instability in the presence of a modest magnetic field gradient.

In the overshoot layer, the presence of a mild turbulence implies that the microscopic values of η and κ should be substituted by their turbulent values in a mean-field description of the system. In other words, if the Alfvén velocity corresponding to the magnetic field is smaller than the turbulent velocity, the turbulent diffusivities have the values derived from the mixing-length theory and their ratio $\eta/\kappa \sim 1$, so that any doubly diffusive instability is virtually suppressed (cf. Schmitt & Rosner 1983; Hughes 2007).

On the other hand, in the presence of a strong magnetic field, we expect the maximum impact on our model because the turbulent diffusivities are strongly quenched, become anisotropic, and strongly dependent on the value of the field itself. Their values could be predicted by numerical models that, however, are many orders of magnitude away from the hydromagnetic regimes characteristic of stars (cf. Käpylä et al. 2020). In view of the simplifications already introduced in Eq. (B.1), we adopt the analytic first-order theory proposed by Kitchatinov et al. (1994) and use it to compute the quenching of η and κ by a magnetic field when the Alfvén velocity V_A is larger than the turbulent velocity u_t . We chose to limit our analysis to the isotropic components of the corresponding η and κ tensors in the regime $V_A/u_t \gg 1$ and conservatively adopt the maximum vertical velocity of the downdrafts as the order of magnitude of the turbulent velocity u_t . For the specific parameter values we adopt for WASP-18 (see Sects. 3.1 and 3.2), we find that the mean value of the magnetic field at the threshold for the doubly diffusive instability increases by a factor of ~ 5 when we take into account the increase in the sub-adiabaticity produced by the reduction in the filling factor of the downdrafts due to the equilibrium tide. Therefore, we confirm the result found with the slender flux tube model that a reduction in the downdraft filling factor leads to a remarkably higher threshold for the instability of the field in the overshoot layer.

Another destabilising mechanism that can act on a magnetic layer is represented by overstable oscillations. They are triggered

by an increase in the field intensity with height when $\eta < \kappa$ and the density stratification across the magnetic layer can be neglected (Hughes 2007). Therefore, they are likely not to be relevant for our model because they require a field gradient that is opposite to that established by the turbulent pumping by the downdrafts that pushes the field downwards thus tending to amplify it towards greater depths.

A final point to be considered is the influence of the tidal shear on the stability of our continuous magnetic field in the overshoot layer or, from a more general point of view, of a toroidal field in the bulk of the convection zone. Unfortunately, the magnetic field instabilities produced by a shear flow parallel to the field and having a velocity gradient in the orthogonal direction are functions of the specific dependence of the velocity on the depth (cf. Hughes 2007), so that no general criterion can be found. Nevertheless, the shear associated with the tidal flow in WASP-18, that is, $\partial\xi_\phi/\partial r$, is about three orders of magnitude smaller than the shear associated with the stellar differential rotation, assuming a radial gradient of the stellar angular velocity in its overshoot layer similar to that of the solar tachocline. A similar conclusion is reached in the case of the convective flows in the bulk of the convection zone. Therefore, we conclude that the effect of the tidal shear on the field stability is likely to be negligible.